ACS Medicinal Chemistry Letters

Technology Note

pubs.acs.org/acsmedchemlett

Kinetic Profile of Amyloid Formation in the Presence of an Aromatic Inhibitor by Nuclear Magnetic Resonance

Gai Liu, Jennifer C. Gaines, Kevin J. Robbins, and Noel D. Lazo*

Carlson School of Chemistry and Biochemistry, Clark University, 950 Main Street, Worcester, Massachusetts 01610, United States

Supporting Information

ABSTRACT: The self-assembly of amyloid proteins into β-sheet rich assemblies is associated with human amyloidoses including Alzheimer's disease, Parkinson's disease, and type 2 diabetes. An attractive therapeutic strategy therefore is to develop small molecules that would inhibit protein self-assembly. Natural polyphenols are potential inhibitors of β-sheet formation. How these compounds affect the kinetics of self-assembly studied by thioflavin T (ThT) fluorescence is not understood primarily because their presence interferes with ThT fluorescence. Here, we show that by plotting peak intensities from nuclear magnetic resonance (NMR) against incubation time, kinetic profiles in the presence of the polyphenol can be obtained from which kinetic parameters of self-assembly can be easily determined. In applying this technique to the self-assembly of the islet amyloid polypeptide in the presence of curcumin, a biphenolic compound found in turmeric, we show that the kinetic profile is atypical in that it shows a prenucleation period during which there is no observable decrease in NMR peak intensities.

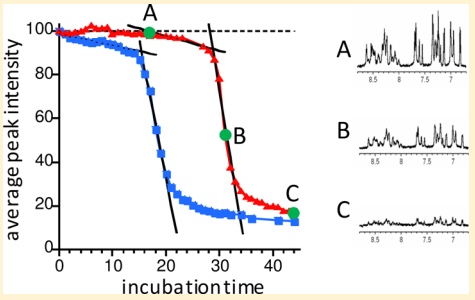

KEYWORDS: *amyloid, ThT fluorescence, curcumin, NMR*

A total of 27 proteins have been identified to form the extracellular β-sheet containing amyloid fibrils associated with human amyloidoses.[1] These include the amyloid-β protein (Aβ) in Alzheimer's disease, α-synuclein in Parkinson's disease, and the islet amyloid polypeptide (IAPP) in type 2 diabetes (T2D). In spite of the large differences in the primary structure of the precursor proteins, the mature fibrils possess common characteristics including unbranched, 10 nm wide morphology as determined by electron microscopy, the ability to bind Congo red and exhibit green birefringence, and X-ray diffraction patterns consistent with cross-β-sheet.[1] Mechanistic studies of fibril formation in hydro have shown that Aβ, α-synuclein, and IAPP undergo a random coil to β-sheet conformational transition.[2]

IAPP is a 37-residue polypeptide (Figure 1A) that is cosecreted with insulin by β-cells of the islets of Langerhans in the pancreas. Molecular biological, biophysical, and genetic evidence support a central role for IAPP in β-cell death and dysfunction associated with T2D.[3,4] The progressive formation of islet amyloid leads to a decrease in β-cell mass.[5] The toxicity of fibrillar IAPP was first demonstrated in the early 1990s,[6] but more recent studies suggest that oligomeric assemblies could be the proximate cytotoxic species in T2D.[3,7] A number of mechanisms behind the toxicity of IAPP oligomers have been proposed,[8] but recent biophysical studies have focused on the ability of IAPP to disrupt model membranes, as reviewed recently.[3] A missense mutation involving the substitution of serine at position 20 with glycine (Figure 1A) has been linked to an early onset, more severe form of T2D.[9] The mutant polypeptide aggregates faster[10,11] and is more toxic than wild-type IAPP.[10] Together, these findings suggest that molecules that significantly delay or completely inhibit IAPP self-assembly are attractive therapeutics for T2D.

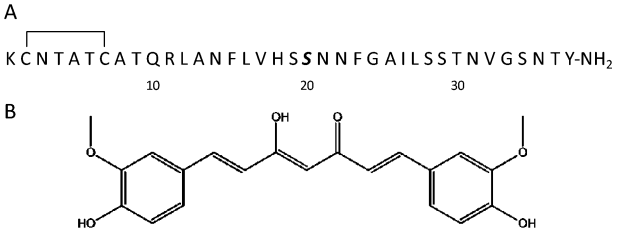

Figure 1. (A) Primary structure of IAPP. The substitution of serine at position 20 by glycine leads to early onset T2D.[9] (B) Curcumin, a biphenol found in the Indian spice turmeric, exists in solution as a keto−enol tautomer.[22]

The self-assembly of monomeric proteins to fibrils may be mediated by nucleation.[12] The overall process is described in quantitative terms by a nucleation period (t_{NP}) during which the nucleus, composed of polypeptide chains arranged in a manner that resembles the aggregated conformation,[12] is formed and by a maximal rate of self-assembly (k_{max}) at which the protein is converted to fibrils. Measurements of t_{NP} and k_{max} have been done primarily with the aid of thioflavin T (ThT) fluorescence. The structural basis for ThT fluorescence

Received: June 8, 2012
Accepted: August 28, 2012
Published: August 28, 2012

is simple: fluorescence is enhanced in the presence of β-sheet-containing fibrils.[13,14] Thus, the plot of fluorescence intensity versus time often has a sigmoidal shape;[15,16] that is, during the lag time, ThT fluorescence is weak, but once the nucleus is formed, fluorescence is enhanced as fibrils form and elongate. ThT fluorescence, however, can be biased when used in the presence of inhibitors that contain fluorescent aromatic groups,[17] making the determination of t_{NP} and k_{max} impossible. A group of compounds that has been studied as potential inhibitors is the natural polyphenols such as those found in tea [e.g., (−)-epigallocatechin-3-gallate[18]], wine (e.g., resveratrol[19]), and spices (e.g., curcumin[20]). The phenolic groups of these compounds are chromophoric and fluorescent.[21] Four mechanisms have been proposed by which these compounds bias ThT fluorescence: quenching of ThT fluorescence by absorbing the light for ThT excitation, direct interference with ThT fluorescence by fluorescing in the same region where ThT fluoresces, interactions between ThT and polyphenol, and competition between ThT and polyphenol for the binding sites on the amyloid assemblies.[17] Here, we use ^{1}H nuclear magnetic resonance (NMR) to determine the kinetic profile of the self-assembly of IAPP in the presence of curcumin and show that it is atypical relative to that of inhibitor-free IAPP in that it includes a prenucleation period.

Curcumin [aka 1,7-bis(4-hydroxy-3-methoxyphenyl)-1,6-heptadiene-3,5-dione], present in the Indian spice turmeric, is used in traditional medicine for its antioxidant, anti-inflammatory, and anticarcinogenic effects. It exists in solution as a keto−enol tautomer (Figure 1B).[22] Its stability depends on pH and temperature. At 37 °C, curcumin decomposes rapidly in neutral and basic solutions, but in acidic conditions, its half-life increases by 2 orders of magnitude.[23] Necula and co-workers showed that curcumin inhibits the oligomerization but not the fibrillization of Aβ(1−42).[24] Daval and co-workers demonstrated that curcumin significantly reduces fibril formation by IAPP in pure buffer.[20] Barry and co-workers showed that curcumin induces alterations in membrane structure,[25] suggesting that the biphenol may also modulate the membrane-assisted self-assembly of IAPP. The small molecule is most efficient when present at a 1:1 ratio (mol:mol), suggesting that it interacts with the monomeric state of the protein or with an assembly formed in the early stages of self-assembly.[26,27] More recently, we showed that curcumin modulates the self-assembly of IAPP by unfolding α-helix.[28]

Because of its insolubility in water, curcumin stock solutions were prepared in 100% ethanol. For control, we investigated the effect of ethanol on the self-assembly of IAPP using circular dichroism (CD). Three samples in 50 mM KH_2PO_4 and 100 mM KCl (pH 5.4) were investigated as follows: IAPP only, IAPP plus curcumin in ethanol [IAPP:curcumin ratio of 1:1 (mol:mol)], and IAPP plus the same amount of ethanol used in the sample with curcumin (1.1% by volume). The acidic pH mimics the acidic environment of IAPP in secretory granules.[11] Figure 2 presents the dichroic spectra acquired for the three samples. Both the IAPP only and the IAPP plus ethanol samples contain β-sheets after 1 day of incubation. The sample with curcumin, on the other hand, remained unstructured up to several days of incubation. Together, these results indicate that the delay in the self-assembly of IAPP in the presence of curcumin in ethanol is due solely to the biphenol.

NMR samples consisting of IAPP only or IAPP plus curcumin in ethanol [IAPP:curcumin ratio of 1:1 (mol:mol)] were then prepared, and a series of one-dimensional ^{1}H NMR spectra were recorded with incubation time at 4 °C. Figure 3A

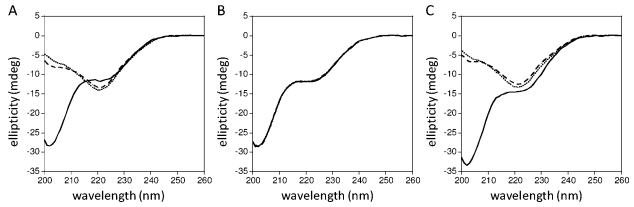

Figure 2. Conformational changes in the self-assembly of IAPP in 50 mM KH_2PO_4 and 100 mM KCl at pH 5.4 by CD at 4 °C. Far-UV CD spectra of (A) IAPP only, (B) IAPP plus curcumin in ethanol [IAPP:curcumin ratio is 1:1 (mol:mol)], and (C) IAPP plus the same amount of ethanol present in panel B. Spectra were taken immediately after sample preparation (solid line), after 1 day of incubation (dashed line), and after 5 days of incubation (dotted line). In panel B, the three spectra overlap. The concentration of IAPP in the three samples is 45 μM. All samples were stored at 4 °C in between the acquisition of spectra.

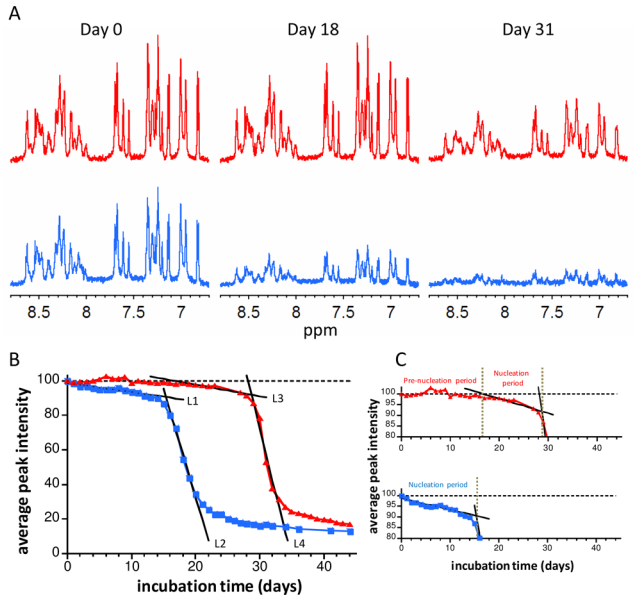

Figure 3. Kinetics of the self-assembly of IAPP by solution-state ^{1}H NMR. (A) Portions of 1D ^{1}H NMR spectra of IAPP in the presence (red) and absence (blue) of curcumin. As self-assembly occurs, the intensities of the peaks in the amide and aromatic regions decrease. (B, C) Kinetic profiles (plots of the average peak intensity vs incubation time) for the self-assembly of IAPP in the absence (blue) and presence (red) of curcumin. The profile without curcumin includes a period where the average peak intensity slowly decreases starting at day 0 followed by a period characterized by a rapid decrease in intensity. Results of best linear fits ($y = mx + b$) are as follows: L1, $m = -0.69$, $b = 100$, and $R^2 = 0.91$; and L2, $m = -12.2$, $b = 276$, and $R^2 = 0.99$. The lag time without curcumin is the time at which lines L1 and L2 intersect, i.e., $t_{NP} = 15.3$ days. The profile with curcumin includes a prenucleation period where the peak intensity does not change until day 17, a period where the average peak intensity slowly decreases, and a period where the peak intensity decreases rapidly. Results of best linear fits are as follows: L3, $m = -0.67$, $b = 111$, and $R^2 = 0.92$; and L4, $m = -15.1$, $b = 527$, and $R^2 = 0.96$. The nucleation period in the presence of curcumin is the time at which lines L3 and L4 intersect minus the prenucleation period, i.e., $t_{NP} = 12.1$ days. The concentration of IAPP in both samples is 45 μM. All samples were kept at 4 °C in between acquisition of spectra.

dx.doi.org/10.1021/ml300147m | ACS Med. Chem. Lett. 2012, 3, 856−859

presents the amide and aromatic regions of spectra acquired immediately after sample preparation (day 0) and at the halfway point of self-assembly as suggested by peak intensities ca. 50% of initial values (day 18 and day 31 for the samples in the absence and presence of curcumin, respectively). We noted that the peak intensities in the sample with curcumin decreased slower than the sample without the small molecule. This result is similar to that we reported previously for the self-assembly of IAPP in 10 mM NaH_2PO_4 (pH 4.3).[28] Together, our results show that the effect of curcumin on the self-assembly of IAPP does not depend on buffer properties such as composition and extent of acidity.

We then determined the averaged normalized peak intensities in the backbone amide, side chain amide, and methyl regions and plotted them against incubation time (Figure 3B). We excluded the aromatic region in the analysis because peaks due to curcumin are found in this region. The basis for using NMR peak intensities in kinetic studies of peptide self-assembly is simple in that as self-assembly occurs, the intensities of peaks due to monomer decrease as a result of the conversion of the NMR-visible monomer to NMR-invisible assemblies.[11,28,29] The decay of average peak intensities with time in the IAPP only sample (blue) and in the IAPP + curcumin sample (red) are inverted sigmoidal plots (Figure 3B,C). The average peak intensity in the sample without curcumin slowly decreased starting at day 0 up to day 15, followed by a much more rapid decrease from day 16 to day 22. In sharp contrast, the average peak intensity in the sample with curcumin does not decrease until day 17, indicating the absence of self-assembly. We call this period the prenucleation period (Figure 3C). Mass spectrometry of a sample of curcumin in phosphate buffer at acidic pH incubated at 4 °C for up to 14 days showed an intense peak due to the curcumin−Na^+ ion (Figure S1 in the Supporting Information), indicating that the intact molecule is responsible for this period. We also studied the self-assembly of IAPP(11−25)[11,30] containing the S20G mutation by two-dimensional NMR (Figure S2 in the Supporting Information). The TOCSY cross-peak volumes in the absence of curcumin decrease starting at day 0, while in the presence of curcumin, the cross-peak volumes did not change for several days. Together, our results suggest that curcumin diminishes the likelihood of nucleation for fibril formation by IAPP in the absence of the polyphenol. Nucleation may involve the formation of α-helix[2,11,30] that is unfolded by curcumin.[28]

Curcumin does not, however, prevent the formation of NMR-invisible assemblies. Figure 3B,C shows that the average peak intensity of IAPP in the presence of curcumin slowly decreased starting on day 17 up to day 29. This was followed by a rapid decrease in peak intensity. Transmission electron microscopy of the NMR samples shows that IAPP in the presence of curcumin also forms fibrils (Figure S3 in the Supporting Information). In studies of potential small-molecule inhibitors of Aβ42 self-assembly, curcumin was classified as a compound that inhibits oligomers on-pathway to fibrils but not fibril formation, suggesting that more than one pathway to fibrils exists.[24] Our work indicates that this classification of curcumin also applies to IAPP self-assembly and that more than one pathway to fibril formation by IAPP also exists.

We then calculated t_{NP} and k_{max} from the kinetic profiles shown in Figure 3B. The determination of these parameters is challenging because of the stochastic nature of nuclei formation resulting in values that scatter significantly. Also, it is important to remove all preaggregated polypeptides, which act as seeds thereby hastening self-assembly. Because we see monomer peaks due to IAPP (Figure 3A), which decrease in intensity with self-assembly, and because we see a long prenucleation period in IAPP self-assembly with curcumin (Figure 3C), the disaggregation protocol that we used that includes pretreatment with hexafluoroisopropanol to dissolve preexisting aggregates, as used by others,[31] is stringent. Results of the best linear fits of the linear regions of the kinetic profiles of IAPP in the absence and presence of curcumin are shown in Figure 3B,C. We define t_{NP} of IAPP self-assembly in the absence and presence of curcumin as the time where lines L1 and L2 intersect and the time where lines L3 and L4 intersect minus the prenucleation period, respectively. The kinetic parameter k_{max} is the maximal rate of decrease in peak intensities, that is, maximal rate of self-assembly to NMR-invisible assemblies. Values of k_{max} are given by the negative of the slopes of lines L2 and L4 for IAPP self-assembly in the absence and presence of curcumin, respectively. Table 1 summarizes the kinetic parameters obtained herein.

Table 1. Kinetic Parameters for the Self-Assembly of IAPP in the Absence and Presence of Curcumin (1:1, mol:mol)

system	prenucleation period (days)	t_{NP} (days)	k_{max} (day^{-1})
IAPP only	0	15.3	12.2
IAPP + curcumin	17	12.1	15.1

Intriguingly, our results show that the product $t_{NP} \times k_{max}$ is constant for IAPP in the absence and presence of curcumin. Analysis of kinetic data from the self-assembly of proteins with dissimilar sequences under considerably different conditions by Fändrich showed that $t_{NP} \times k_{max}$ from fluorescence is approximately equal to a constant parameter α.[32] Although the values of t_{NP} and k_{max} change significantly with primary structure and experimental conditions, α is much less affected by these variables. Fändrich noted that similarities in α indicate that the effective sizes of nuclei in aggregating systems are similar. It will be interesting to find out, therefore, if our finding that $t_{NP} \times k_{max}$ from NMR is also equal to a constant parameter applies to a much wider range of samples and conditions.

Kinetic profiles and kinetic parameters for self-assembly, important in the evaluation of the efficacy of potential inhibitors, can be easily determined from inverted sigmoidal plots obtained by plotting normalized NMR peak intensities against time. This method overcomes problems associated with kinetic studies of protein self-assembly in the presence of fluorescent small molecules by ThT fluorescence.

■ ASSOCIATED CONTENT

Supporting Information

Materials and methods, mass spectrum of curcumin in phosphate buffer, two-dimensional NMR data for IAPP(11−25) containing the S20G mutation, and electron micrographs. This material is available free of charge via the Internet at http://pubs.acs.org.

■ AUTHOR INFORMATION

Corresponding Author

*E-mail: nlazo@clarku.edu.

Funding

This work was supported by the Carlson Endowed Chair to N.D.L.

Notes

The authors declare no competing financial interest.

■ ACKNOWLEDGMENTS

We thank Dr. Guoxing Lin for the maintenance of the NMR spectrometer used in this work and Veli Selmani and Stephanie Maniatis for mass spectrometry.

■ REFERENCES

(1) Sipe, J. D.; Benson, M. D.; Buxbaum, J. N.; Ikeda, S.; Merlini, G.; Saraiva, M. J.; Westermark, P. Amyloid fibril protein nomenclature: 2010 recommendations from the nomenclature committee of the International Society of Amyloidosis. *Amyloid* **2010**, *17*, 101−104.

(2) Abedini, A.; Raleigh, D. P. A critical assessment of the role of helical intermediates in amyloid formation by natively unfolded proteins and polypeptides. *Protein Eng., Des. Sel.* **2009**, *22*, 453−459.

(3) Brender, J. R.; Salamekh, S.; Ramamoorthy, A. Membrane disruption and early events in the aggregation of the diabetes related peptide IAPP from a molecular perspective. *Acc. Chem. Res.* **2012**, *45*, 454−462.

(4) Hebda, J. A.; Miranker, A. D. The interplay of catalysis and toxicity by amyloid intermediates on lipid bilayers: insights from type II diabetes. *Annu. Rev. Biophys.* **2009**, *38*, 125−152.

(5) Westermark, P.; Wilander, E. The influence of amyloid deposits on the islet volume in maturity onset diabetes mellitus. *Diabetologia* **1978**, *15*, 417−421.

(6) Lorenzo, A.; Razzaboni, B.; Weir, G. C.; Yankner, B. A. Pancreatic islet cell toxicity of amylin associated with type-2 diabetes mellitus. *Nature* **1994**, *368*, 756−760.

(7) Zraika, S.; Hull, R. L.; Verchere, C. B.; Clark, A.; Potter, K. J.; Fraser, P. E.; Raleigh, D. P.; Kahn, S. E. Toxic oligomers and islet β cell death: guilty by association or convicted by circumstantial evidence? *Diabetologia* **2010**, *53*, 1046−1056.

(8) Westermark, P.; Andersson, A.; Westermark, G. T. Islet amyloid polypeptide, islet amyloid, and diabetes mellitus. *Physiol. Rev.* **2011**, *91*, 795−826.

(9) Sakagashira, S.; Sanke, T.; Hanabusa, T.; Shimomura, H.; Ohagi, S.; Kumagaye, K. Y.; Nakajima, K.; Nanjo, K. Missense mutation of amylin gene (S20G) in Japanese NIDDM patients. *Diabetes* **1996**, *45*, 1279−1281.

(10) Sakagashira, S.; Hiddinga, H. J.; Tateishi, K.; Sanke, T.; Hanabusa, T.; Nanjo, K.; Eberhardt, N. L. S20G mutant amylin exhibits increased in vitro amyloidogenicity and increased intracellular cytotoxicity compared to wild-type amylin. *Am. J. Pathol.* **2000**, *157*, 2101−2109.

(11) Liu, G.; Prabhakar, A.; Aucoin, D.; Simon, M.; Sparks, S.; Robbins, K. J.; Sheen, A.; Petty, S. A.; Lazo, N. D. Mechanistic studies of peptide self-assembly: Transient α-helices to stable β-sheets. *J. Am. Chem. Soc.* **2010**, *132*, 18223−18232.

(12) Harper, J. D.; Lansbury, P. T., Jr. Models of amyloid seeding in Alzheimer's disease and scrapie: mechanistic truths and physiological consequences of the time-dependent solubility of amyloid proteins. *Annu. Rev. Biochem.* **1997**, *66*, 385−407.

(13) Groenning, M.; Olsen, L.; van de Weert, M.; Flink, J. M.; Frokjaer, S.; Jorgensen, F. S. Study on the binding of Thioflavin T to β-sheet-rich and non-β-sheet cavities. *J. Struct. Biol.* **2007**, *158*, 358−369.

(14) Robbins, K. J.; Liu, G.; Lin, G.; Lazo, N. D. Detection of strongly bound Thioflavin T species in amyloid fibrils by ligand-detected ^{1}H NMR. *J. Phys. Chem. Lett.* **2011**, *2*, 735−740.

(15) Xue, W. F.; Homans, S. W.; Radford, S. E. Systematic analysis of nucleation-dependent polymerization reveals new insights into the mechanism of amyloid self-assembly. *Proc. Natl. Acad. Sci. U.S.A.* **2008**, *105*, 8926−8931.

(16) Auer, S.; Kashchiev, D. Insight into the correlation between lag time and aggregation rate in the kinetics of protein aggregation. *Proteins* **2010**, *78*, 2412−2416.

(17) Hudson, S. A.; Ecroyd, H.; Kee, T. W.; Carver, J. A. The thioflavin T fluorescence assay for amyloid fibril detection can be biased by the presence of exogenous compounds. *FEBS J.* **2009**, *276*, 5960−5972.

(18) Meng, F.; Abedini, A.; Plesner, A.; Verchere, C. B.; Raleigh, D. P. The flavanol (−)-epigallocatechin 3-gallate inhibits amyloid formation by islet amyloid polypeptide, disaggregates amyloid fibrils, and protects cultured cells against IAPP-induced toxicity. *Biochemistry* **2010**, *49*, 8127−8133.

(19) Mishra, R.; Sellin, D.; Radovan, D.; Gohlke, A.; Winter, R. Inhibiting islet amyloid polypeptide fibril formation by the red wine compound resveratrol. *Chembiochem* **2009**, *10*, 445−9.

(20) Daval, M.; Bedrood, S.; Gurlo, T.; Huang, C. J.; Costes, S.; Butler, P. C.; Langen, R. The effect of curcumin on human islet amyloid polypeptide misfolding and toxicity. *Amyloid* **2010**, *17*, 118−128.

(21) Kunwar, A.; Barik, A.; Pandey, R.; Priyadarsini, K. I. Transport of liposomal and albumin loaded curcumin to living cells: An absorption and fluorescence spectroscopic study. *Biochim. Biophys. Acta* **2006**, *1760*, 1513−1520.

(22) Payton, F.; Sandusky, P.; Alworth, W. L. NMR study of the solution structure of curcumin. *J. Nat. Prod.* **2007**, *70*, 143−146.

(23) Wang, Y. J.; Pan, M. H.; Cheng, A. L.; Lin, L. I.; Ho, Y. S.; Hsieh, C. Y.; Lin, J. K. Stability of curcumin in buffer solutions and characterization of its degradation products. *J. Pharm. Biomed. Anal.* **1997**, *15*, 1867−1876.

(24) Necula, M.; Kayed, R.; Milton, S.; Glabe, C. G. Small molecule inhibitors of aggregation indicate that amyloid β oligomerization and fibrillization pathways are independent and distinct. *J. Biol. Chem.* **2007**, *282*, 10311−10324.

(25) Barry, J.; Fritz, M.; Brender, J. R.; Smith, P. E.; Lee, D. K.; Ramamoorthy, A. Determining the effects of lipophilic drugs on membrane structure by solid-state NMR spectroscopy: The case of the antioxidant curcumin. *J. Am. Chem. Soc.* **2009**, *131*, 4490−4498.

(26) Hafner-Bratkovic, I.; Gaspersic, J.; Smid, L. M.; Bresjanac, M.; Jerala, R. Curcumin binds to the α-helical intermediate and to the amyloid form of prion protein—A new mechanism for the inhibition of PrP^{Sc} accumulation. *J. Neurochem.* **2008**, *104*, 1553−1564.

(27) Mishra, R.; Bulic, B.; Sellin, D.; Jha, S.; Waldmann, H.; Winter, R. Small-molecule inhibitors of islet amyloid polypeptide fibril formation. *Angew. Chem., Int. Ed. Engl.* **2008**, *47*, 4679−4682.

(28) Sparks, S.; Liu, G.; Robbins, K. J.; Lazo, N. D. Curcumin modulates the self-assembly of the islet amyloid polypeptide by disassembling α-helix. *Biochem. Biophys. Res. Commun.* **2012**, *422*, 551−555.

(29) Mishra, R.; Geyer, M.; Winter, R. NMR spectroscopic investigation of early events in IAPP amyloid fibril formation. *Chembiochem* **2009**, *10*, 1769−72.

(30) Liu, G.; Robbins, K. J.; Sparks, S.; Selmani, V.; Bilides, K. M.; Gomes, E. E.; Lazo, N. D. Helix-dipole effects in peptide self-assembly to amyloid. *Biochemistry* **2012**, *51*, 4167−4174.

(31) O'Nuallain, B.; Williams, A. D.; Westermark, P.; Wetzel, R. Seeding specificity in amyloid growth induced by heterologous fibrils. *J. Biol. Chem.* **2004**, *279*, 17490−17499.

(32) Fändrich, M. Absolute correlation between lag time and growth rate in the spontaneous formation of several amyloid-like aggregates and fibrils. *J. Mol. Biol.* **2007**, *365*, 1266−1270.